# Horizons as boundary conditions in spherical symmetry

Sharmila Gunasekaran* and Ivan Booth†

*Department of Mathematics and Statistics Memorial University of Newfoundland St. John's, Newfoundland and Labrador, A1C 5S7, Canada*

(Received 27 May 2019; published 10 September 2019)

We initiate the development of a horizon-based initial (or rather final) value formalism to describe the geometry and physics of the near-horizon spacetime: data specified on the horizon and a future ingoing null boundary determine the near-horizon geometry. In this initial paper we restrict our attention to spherically symmetric spacetimes made dynamic by matter fields. We illustrate the formalism by considering a black hole interacting with a) inward-falling, null matter (with no outward flux) and b) a massless scalar field. The inward-falling case can be exactly solved from horizon data. For the more involved case of the scalar field we analytically investigate the near slowly evolving horizon regime and propose a numerical integration for the general case.

DOI: 10.1103/PhysRevD.100.064019

## I. INTRODUCTION

This paper begins an investigation into what horizon dynamics can tell us about external black hole physics. At first thought this might seem obvious: if one watches a numerical simulation of a black hole merger and sees a post-merger horizon ringdown (see e.g., Ref. [1]) then it is natural to think of that oscillation as a source of emitted gravitational waves. However this cannot be the case. Neither event nor apparent horizons can actually send signals to infinity: apparent horizons lie inside event horizons which in turn are the boundary for signals that can reach infinity [2]. It is not horizons themselves that interact but rather the "near-horizon" fields. This idea was (partially) formalized as a "stretched horizon" in the membrane paradigm [3].

Then the best that we can hope for from horizons is that they act as a proxy for the near-horizon fields with horizon evolution reflecting some aspects of their dynamics. As explored in Refs. [4–8] there should then be a correlation between horizon evolution and external, observable, black hole physics.

Robinson-Trautman spacetimes (see e.g., Ref. [9]) demonstrate that this correlation cannot be perfect. In those spacetimes there can be outgoing gravitational (or other) radiation arbitrarily close to an isolated (equilibrium) horizon [10]. Hence our goal is twofold: to understand the conditions under which a correlation will exist and to learn precisely what information it contains.

The idea that horizons should encode physical information about black hole physics is not new. The classical definition of a black hole as the complement of the causal past of future null infinity [2] is essentially global and so defines a black hole spacetime rather than a black hole *in* some spacetime. However there are also a range of geometrically defined black hole boundaries based on outer and/or marginally trapped surfaces that seek to localize black holes. These include apparent [2], trapping [11], isolated [10,12–14] and dynamical [15] horizons as well as future holographic screens [16]. These quasilocal definitions of black holes have successfully localized black hole mechanics to the horizon [11–13,15–17] and been particularly useful in formalizing what it means for a (localized) black hole to evolve or be in equilibrium. They are used in numerical relativity not only as excision surfaces (see, e.g., the discussions in Refs. [18,19]) but also in interpreting physics (see e.g., Refs. [4–8,20–24]).

In this paper we work to quantitatively link horizon dynamics to observable black hole physics. To establish an initial framework and build intuition we for now restrict our attention to spherically symmetric marginally outer trapped tubes (MOTTs) in similarly symmetric spacetimes. Matter fields are included to drive the dynamics. Our primary approach is to take horizon data as a (partial) final boundary condition that is used to determine the fields in a region of spacetime in its causal past. In particular these boundary conditions constrain the geometry and physics of the associated "near-horizon" spacetime. The main application that we have in mind is interpreting the physics of evolving horizons that have been generated by either numerical simulations or theoretical considerations.

Normally, data on a MOTT by itself is not sufficient to specify any region of the external spacetime. As shown in Fig. 1(a) even for a spacelike MOTT (a dynamical horizon) the region determined by a standard $(3+1)$ initial value

*sdgg82@mun.ca
†ibooth@mun.ca

 

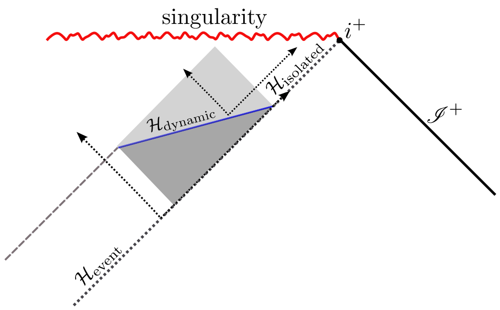


(a)Future and past domains of dependence for $\mathcal{H}_{\rm dynamic}$: standard (3+1) IVP

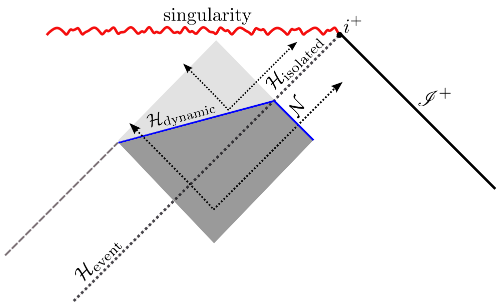


(b)Future and past domains of dependence for $\mathcal{H}_{\rm dynamic} \cup \mathcal{N}$: characteristic IVP

FIG. 1. Domains of dependence of initial data.

formulation would lie entirely within the event horizon. More information is needed to determine the near-horizon spacetime and hence in this paper we work with a characteristic initial value formulation [25–29] where extra data is specified on a null surface $\mathcal{N}$ that is transverse to the horizon [Fig. 1(b)]. Intuitively the horizon records inward-moving information while $\mathcal{N}$ records the outward-moving information. Together they are sufficient to reconstruct the spacetime.

Many works have studied spacetime near horizons; however they have not exactly addressed this problem. Most works focused on isolated horizons. References [30] and [31] examined spacetime near an isolated extremal horizon as a Taylor series expansion of the horizon while Refs. [32] and [33] studied spacetime near more general isolated horizons but in a characteristic initial value formulation with the extra information specified on a transverse null surface. Reference [34] studied both the isolated and dynamical case though again as a Taylor series expansion off the horizon. In the case of the Taylor expansions, as one goes to higher and higher orders one needs to know higher- and higher-order derivatives of metric quantities at the horizon to continue the expansion. While the current paper instead investigates the problem as a final value problem, it otherwise closely follows the notation of and uses many results from Ref. [34].

This paper is organized as follows. We introduce the final value formulation of spherically symmetric general relativity in Sec. II. We illustrate this for infalling null matter in Sec. III and then the much more interesting massless scalar field in Sec. IV. We conclude with a discussion of results in Sec. V.

## II. FORMULATION

### A. Coordinates and metric

We work in a spherically symmetric spacetime $(\mathcal{M}, g)$ and a coordinate system whose nonangular coordinates are $\rho$ (an ingoing affine parameter) and $v$ (which labels the ingoing null hypersurfaces and increases into the future). Hence, $g_{\rho\rho} = 0$ and the curves tangent to the future-oriented inward-pointing

$$N = \frac{\partial}{\partial\rho} \tag{1}$$

are null. We then scale $v$ so that $\mathcal{V} = \frac{\partial}{\partial v}$ satisfies

$$\mathcal{V} \cdot N = -1. \tag{2}$$

One coordinate freedom still remains: the scaling of the affine parameter on the individual null geodesics

$$\tilde{\rho} = f(v)\rho. \tag{3}$$

In Sec. II C we will fix this freedom by specifying how $N$ is to be scaled along the $\rho = 0$ surface $\Sigma$ (which we take to be a black hole horizon).

Next we define the future-oriented outward-pointing null normal to the spherical surfaces $S_{(v,\rho)}$ as $\ell^a$ and scale so that

$$\ell \cdot N = -1. \tag{4}$$

With this choice the four-metric $g_{ab}$ and induced two-metric $\tilde{q}_{ab}$ on the $S_{(v,\rho)}$ are related by

$$g^{ab} = \tilde{q}^{ab} - \ell^a N^b - N^a \ell^b. \tag{5}$$

Further for some function $C$ we can write

$$\mathcal{V} = \ell - CN. \tag{6}$$

The coordinates and normal vectors are depicted in Fig. 2 and give the following form of the metric:

$$ds^2 = 2C(v,\rho)\mathrm{d}v^2 - 2\mathrm{d}v\mathrm{d}\rho + R(v,\rho)^2\mathrm{d}\Omega^2 \tag{7}$$

where $R(v,\rho)$ is the areal radius of the $S_{(v,\rho)}$ surfaces. Note the similarity to ingoing Eddington-Finkelstein coordinates for a Schwarzschild black hole. However $\partial/\partial\rho$ points inwards as opposed to the outward-oriented $\partial/\partial r$ in those coordinates (hence the negative sign on the $\mathrm{d}v\mathrm{d}\rho$ cross term).

Typically, as shown in Fig. 2 we will be interested in regions of spacetime that are bordered in the future by a surface $\Sigma$ of indeterminate sign on which $\rho = 0$ and a null

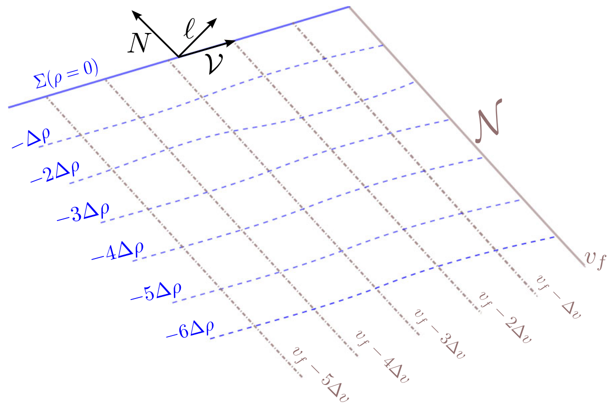


FIG. 2. Coordinate system for characteristic evolution. We work with final boundary conditions so that in the region of interest $\rho < 0$.

$\mathcal{N}$ which is one of the $v = \text{const}$ surfaces (and so $\rho < 0$ in the region of interest). We will explore how data on those surfaces determines the region of spacetime in their causal past.

### B. Equations of motion

In this section we break up the Einstein equations relative to these coordinates, beginning by defining some geometric quantities that appear in the equations.

First the null expansions for the $\ell^a$ and $N^a$ congruences are

$$\theta_{(\ell)} = \tilde{q}^{ab}\nabla_a \ell_b = \frac{2}{R}\mathcal{L}_\ell R \quad \text{and} \tag{8}$$

$$\theta_{(N)} = \tilde{q}^{ab}\nabla_a N_b = \frac{2}{R}\mathcal{L}_N R = \frac{2}{R}R_{,\rho}, \tag{9}$$

while the inaffinities of the null vector fields are

$$\kappa_N = -N^a N_b \nabla_a \ell^b = 0 \quad \text{and} \tag{10}$$

$$\kappa_{\mathcal{V}} = \kappa_\ell - C\kappa_N = -\ell^a N_b \nabla_a \ell^b. \tag{11}$$

By construction $\kappa_N = 0$ and so we can drop it from our equations and henceforth write

$$\kappa \equiv \kappa_{\mathcal{V}} = \kappa_\ell. \tag{12}$$

Finally the Gaussian curvature of $S_{(v,\rho)}$ is

$$\tilde{K} = \frac{1}{R^2}. \tag{13}$$

Then these curvature quantities are related by constraint equations along the surfaces of constant $\rho$

$$\mathcal{L}_{\mathcal{V}} R = \mathcal{L}_\ell R - C\mathcal{L}_N R \quad \text{(by definition)}, \tag{14}$$

$$\mathcal{L}_{\mathcal{V}}\theta_{(\ell)} = \kappa\theta_{(\ell)} + C\left(\frac{1}{R^2} + \theta_{(N)}\theta_{(\ell)} - G_{\ell N}\right) - \left(G_{\ell\ell} + \frac{1}{2}\theta_{(\ell)}^2\right), \tag{15}$$

$$\mathcal{L}_{\mathcal{V}}\theta_{(N)} = -\kappa\theta_{(N)} - \left(\frac{1}{R^2} + \theta_{(N)}\theta_{(\ell)} - G_{\ell N}\right) + C\left(G_{NN} + \frac{1}{2}\theta_{(N)}^2\right), \tag{16}$$

and "time" derivatives in the $\rho$ direction

$$\mathcal{L}_N\theta_{(N)} = -\frac{\theta_{(N)}^2}{2} - G_{NN}, \tag{17}$$

$$\mathcal{L}_N\theta_{(\ell)} = -\frac{1}{R^2} - \theta_{(N)}\theta_{(\ell)} + G_{\ell N}, \tag{18}$$

$$\mathcal{L}_N\kappa = \frac{1}{R^2} + \frac{1}{2}\theta_{(N)}\theta_{(\ell)} - \frac{1}{2}G_{\tilde{q}} - G_{\ell N}, \tag{19}$$

where by the choice of the coordinates

$$\kappa = \mathcal{L}_N C. \tag{20}$$

These equations can be derived from the variations for the corresponding geometric quantities (see, e.g., Refs. [35] and [34]) and of course are coupled to the matter content of the system through the Einstein equations

$$G_{ab} = 8\pi T_{ab}. \tag{21}$$

Using Eqs. (8) and (9) we can rewrite the constraint and evolution equations in terms of the metric coefficients and coordinates as

$$R_{,v} = R_\ell - CR_N, \tag{22}$$

$$R_{\ell,v} = \kappa R_\ell + \frac{C(1+4R_\ell R_N)}{2R} - \frac{R}{2}(G_{\ell\ell} + CG_{\ell N}), \tag{23}$$

$$R_{N,v} = -\kappa R_N - \frac{(1+4R_\ell R_N)}{2R} + \frac{R}{2}(G_{\ell N} + CG_{NN}), \tag{24}$$

and

$$R_{,\rho\rho} = -\frac{R}{2}G_{NN}, \tag{25}$$

$$(RR_\ell)_{,\rho} = -\frac{1}{2} + \frac{R^2}{2}G_{\ell N}, \tag{26}$$

$$C_{,\rho\rho} = \frac{1}{R^2} + \frac{2R_\ell R_N}{R^2} - \frac{1}{2}G_{\tilde{q}} - G_{\ell N}, \tag{27}$$

where

$$\kappa = C_{,\rho}. \tag{28}$$

For those who do not want to work through the derivations of Refs. [35] and [34], these can also be derived fairly easily (thanks to the spherical symmetry) from an explicit calculation of the Einstein tensor for Eq. (7).

### C. Final data

We will focus on the case where $\rho = 0$ is an isolated or dynamical horizon $H$. Thus

$$\theta_{(\ell)} \overset{H}{=} 0 \Leftrightarrow R_\ell \overset{H}{=} 0. \tag{29}$$

The notation $\overset{H}{=}$ indicates that the equality holds on $H$ (but not necessarily anywhere else). Further we can use the coordinate freedom (3) to set

$$R_N \overset{H}{=} R_{,\rho}| \overset{H}{=} -1. \tag{30}$$

On $H$, the constraints (22)–(24) fix three of

$$\{C, \kappa, R, R_\ell, R_N, G_{\ell\ell}, G_{\ell N}, G_{NN}\} \tag{31}$$

given the other five quantities. For example if $R_\ell \overset{H}{=} 0$ and $R_N \overset{H}{=} -1$ then Eqs. (22) and (23) give

$$R_{,v} \overset{H}{=} C \overset{H}{=} \frac{R^2 G_{\ell\ell}}{1 - R^2 G_{\ell N}} \tag{32}$$

and Eq. (24) gives

$$\kappa = C_\rho \overset{H}{=} \frac{1}{2R} - \frac{R}{2}(G_{\ell N} + C G_{NN}). \tag{33}$$

Thus if $G_{\ell\ell}$ and $G_{\ell N}$ are specified for $v_i \leq v \leq v_f$ on $H$ and $R(v_f) \overset{H}{=} R_f$ then one can solve Eq. (32) to find $R$ over the entire range. Equivalently one could take $R$ and one of $G_{\ell\ell}$ or $G_{\ell N}$ as primary and then solve for the other component of the stress-energy.

Of course, in general the matter terms will also be constrained by their own equations; these will be treated in later sections. Further data on $\rho = 0$ will generally not be sufficient to fully determine the regions of interest and data will also be needed on an $\mathcal{N}$. Again this will depend on the specific matter model.

Nevertheless if there is a MOTT at $\rho = 0$ then the constraints provide significant information about the horizon. If $G_{\ell\ell} = 0$ (no flux of matter through the horizon) then we have an isolated horizon with $C = 0$, a constant $R$ and a null $H$. This is independent of other components of the stress-energy.

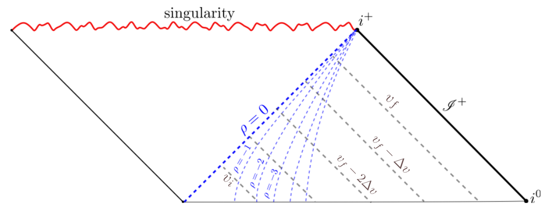


(a) Isolated horizon : $d\rho$ is timelike for all values of $\rho$

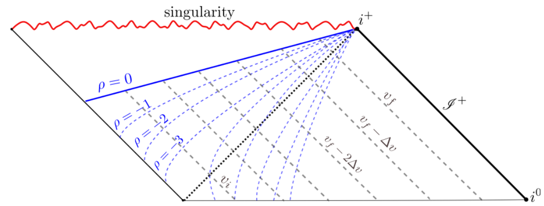


(b) Dynamical horizon : $d\rho$ is spacelike for small values of $\rho$ and eventually becomes timelike for large values of $\rho$

FIG. 3. Spacetime foliation for isolated and dynamical horizons.

Alternatively if $G_{\ell\ell} > 0$ (the energy conditions forbid it to be negative) and $G_{\ell N} < 1/R^2$ then we have a dynamical horizon with $C > 0$, increasing $R$ and spacelike $H$.[1] Note that this growth does not depend in any way on $G_{NN}$: there is no sense in which the growing horizon "catches" outward-moving matter and hence grows even faster. The behavior of the coordinates relative to isolated and dynamical horizons along with $\mathcal{I}^+$ is illustrated in Fig. 3.

The evolution equations are more complicated and depend on the matter field equations. We examine two such cases in the following sections.

## III. TRACELESS INWARD-FLOWING NULL MATTER

As our first example consider matter that falls entirely in the inward $N$ direction with no outward $\ell$ flux. Then data on the horizon should be sufficient to entirely determine the region of spacetime traced by the horizon-crossing inward null geodesics: there are no dynamics that do not involve the horizon.

Translating these words into equations, we assume that

$$T_{ab} N^a N^b = 0 \tag{34}$$

(no matter flows in the outward $\ell$ direction). Further, for simplicity we also assume that it is trace-free

$$g^{ab} T_{ab} = 0 \Leftrightarrow T_{\tilde{q}} = 2 T_{\ell N}. \tag{35}$$

[1] $G_{\ell N} > 1/R^2$ signals that another MOTS has formed outside the original one and so a numerical simulation would see an apparent horizon "jump" [16,36]. In the current paper all matter satisfies $G_{\ell N} < 1/R^2$ and so this situation does not arise.

Then we can solve for the metric using only the Bianchi identities

$$\nabla_a G^{ab} = 0, \tag{36}$$

without any reference to detailed equations of motion for the matter field. Keeping spherical symmetry but temporarily suspending the other simplifying assumptions they may be written as

$$\mathcal{L}_\ell(R^2 G_{NN}) + \mathcal{L}_N(R^2 G_{\ell N}) + R^2(2\kappa_\ell G_{NN}) + \frac{1}{2}R^2\theta_{(N)}G_{\tilde{q}} = 0, \tag{37}$$

$$\mathcal{L}_N(R^2 G_{\ell\ell}) + \mathcal{L}_\ell(R^2 G_{\ell N}) + R^2(-2\kappa_N G_{\ell\ell}) + \frac{1}{2}R^2\theta_{(\ell)}G_{\tilde{q}} = 0. \tag{38}$$

In terms of metric coefficients with $\kappa_N = 0$ plus Eqs. (34) and (35) these reduce to

$$(R^4 G_{\ell N})_{,\rho} = 0 \quad \text{and} \tag{39}$$

$$(R^2 G_{\ell\ell})_{,\rho} + \frac{1}{R^2}(R^4 G_{\ell N})_{,v} = 0. \tag{40}$$

As we shall see, this class of matter includes interesting examples like the Vaidya-Reissner-Nordström solution (charged null dust).

We now demonstrate that given knowledge of $G_{\ell\ell}$ and $G_{\ell N}$ over a region of horizon $\bar{H} = \{H\colon v_i \leq v \leq v_f\}$ as well as $R(v_f) \overset{H}{=} R_f$ we can determine the spacetime everywhere out along the horizon-crossing inward null geodesics.

### A. On the horizon

First consider the constraints on $\bar{H}$. In this case it is tidier to take $R$ and $G_{\ell N}$ as primary. Then we can specify

$$R \overset{H}{=} R_H(v) \quad \text{and} \quad G_{\ell N} \overset{H}{=} \frac{Q(v)}{R_H^4} \tag{41}$$

for some functions $R_H(v)$ (dimensions of length) and $Q_H(v)$ (dimensions of length squared) where the form of the latter is chosen for future convenience. Then

$$C \overset{H}{=} R_{H,v} \tag{42}$$

and by Eq. (32)

$$G_{\ell\ell} \overset{H}{=} R_{H,v}\left(\frac{1}{R_H^2} - \frac{Q}{R_H^4}\right). \tag{43}$$

Finally by Eq. (33),

$$\kappa \overset{H}{=} C_\rho \overset{H}{=} \frac{1}{2R_H}\left(1 - \frac{Q}{R_H^2}\right). \tag{44}$$

### B. Off the horizon

Next, integrate away from $\bar{H}$. First with $G_{NN} = 0$ Eq. (25) can be integrated with initial condition (30) to give

$$R(v,\rho) = R_H(v) - \rho. \tag{45}$$

Then with Eq. (41) we can integrate Eq. (39) to find

$$G_{\ell N} = \frac{Q}{R^4} \tag{46}$$

and use this result and Eq. (43) to integrate Eq. (40) to get

$$G_{\ell\ell} = \frac{(R_H^2 - Q)R_{H,v}}{R_H^2 R^2} + \frac{\rho Q_{,v}}{R_H R^3}. \tag{47}$$

With these results in hand and the initial condition $R_\ell \overset{H}{=} 0$ we integrate Eq. (26) to get

$$R_\ell = \frac{\rho(Q - R_H^2 + \rho R_H)}{2R^2 R_H} \tag{48}$$

and finally with the initial conditions (32) and (33) we can integrate Eq. (27) to find

$$C = R_{H,v} - R_\ell. \tag{49}$$

### C. Comparison with Vaidya-Reissner-Nordström

We can now compare this derivation to a known example. The Vaidya-Reissner-Nordström (VRN) metric takes the form

$$\mathrm{d}s^2 = -\left(1 - \frac{2m(v)}{r} + \frac{q(v)^2}{r^2}\right)\mathrm{d}v^2 + 2\mathrm{d}v\mathrm{d}r + r^2\mathrm{d}\Omega^2 \tag{50}$$

where the apparent horizon $r_H = m + \sqrt{m^2 - q^2}$ and $r$ is an affine parameter of the ingoing null geodesics. To put it into the form of Eq. (7) where the affine parameter measures distance off the horizon we make the transformation

$$r = r_H - \rho \tag{51}$$

whence the metric takes the form

$$\mathrm{d}s^2 = -\left(2r_{H,v} - \frac{\rho(q^2 - r_H(r_H - \rho))}{r_H(r_H - \rho)^2}\right)\mathrm{d}v^2 - 2\mathrm{d}v\mathrm{d}\rho + (r_H - \rho)^2\mathrm{d}\Omega^2. \tag{52}$$

That is

$$C = r_{H,v} - \frac{\rho(q^2 - r_H(r_H - \rho))}{2r_H(r_H - \rho)^2} \tag{53}$$

$$R = r_H - \rho \tag{54}$$

and on the horizon

$$C \overset{H}{=} r_{H,v} \quad \text{and} \quad R \overset{H}{=} r_H \tag{55}$$

as expected.

To do a complete match we calculate the rest of the quantities. First appropriate null vectors are

$$\ell = \frac{\partial}{\partial v} + \left( r_{H,v} - \frac{\rho(q^2 - r_H(r_H - \rho))}{2r_H(r_H - \rho)^2} \right) \frac{\partial}{\partial \rho}, \tag{56}$$

$$N = \frac{\partial}{\partial \rho}. \tag{57}$$

Then direct calculation shows that

$$R_\ell = -\frac{\rho(q^2 - r_H(r_H - \rho))}{2r_H(r_H - \rho)^2}, \tag{58}$$

$$R_N = -1 \tag{59}$$

and

$$G_{\ell\ell} = \frac{(r_H^2 - q^2) r_{H,v}}{r_H^2 r^2} + \frac{2\rho q q_{,v}}{r_H r^3}, \tag{60}$$

$$G_{\ell N} = \frac{q^2}{(r_H - \rho)^2}, \tag{61}$$

$$G_{NN} = 0, \tag{62}$$

$$G_q = \frac{2q^2}{(r_H - \rho)^2}. \tag{63}$$

It is clear that with $R_H = r_H$ and $Q = q^2$ our general results (41)–(49) give rise to the VRN spacetime (as they should).

As expected the data on the horizon is sufficient to determine the spacetime everywhere back out along the ingoing null geodesics: we simply solve a set of (coupled) ordinary differential equations along each curve. With the matter providing the only dynamics and that matter only moving inwards along the geodesics the problem is quite straightforward. In this case there is no need to specify extra data on $\mathcal{N}$.

We now turn to the more interesting case where the dynamics are driven by a scalar field for which there will be both inward and outward fluxes of matter.

## IV. MASSLESS SCALAR FIELD

Spherical spacetimes containing a massless scalar field $\phi(v, \rho)$ are governed by the stress-energy tensor given by,

$$T_{ab} = \nabla_a \phi \nabla_b \phi - \frac{1}{2} g_{ab} \nabla^c \phi \nabla_c \phi. \tag{64}$$

This system has nonvanishing inward and outward fluxes which are,

$$T_{\ell\ell} = (\phi_\ell)^2, \tag{65}$$

$$T_{NN} = (\phi_N)^2. \tag{66}$$

Here and in the following keep in mind that $N = \frac{\partial}{\partial \rho}$ and so $\phi_N = \phi_{,\rho}$. We also observe from Eq. (64) that,

$$T_{\ell N} = 0. \tag{67}$$

These fluxes are related by the wave equation

$$\Box_g \phi \coloneqq \nabla^\alpha \nabla_\alpha \phi = 0 \Rightarrow (R\phi_\ell)_{,\rho} = -R_\ell \phi_{,\rho}. \tag{68}$$

For our purposes we are not particularly interested in the value of $\phi$ itself but rather in the associated net flux of energies in the ingoing and outgoing null direction. Hence we define

$$\Phi_\ell = \sqrt{4\pi} R \phi_\ell \quad \text{and} \quad \Phi_N = \sqrt{4\pi} R \phi_N. \tag{69}$$

Respectively these are the square roots of the scalar field energy fluxes in the $N$ and $\ell$ directions. That is, over a sphere of radius $R$, $\Phi_\ell$ is the square root of the total integrated flux in the $N$ direction and $\Phi_N$ is the square root of the total integrated flux in the $\ell$ direction. Though not strictly correct, we will often refer to $\Phi_\ell$ and $\Phi_N$ themselves as fluxes.

Then Eq. (68) becomes

$$\Phi_{\ell,\rho} = -\frac{R_\ell \Phi_N}{R} \tag{70}$$

or, making use of the fact that $\phi_{,v\rho} = \phi_{,\rho v}$,

$$\Phi_{N,v} = -\kappa \Phi_N - C\Phi_{N,\rho} - \frac{R_N \Phi_\ell}{R}. \tag{71}$$

These can usefully be understood as advection equations with sources. Recall that a general homogeneous advection equation can be written in the form

$$\frac{\partial \psi}{\partial t} + C \frac{\partial \psi}{\partial x} = 0 \tag{72}$$

where $C$ is the speed of flow of $\psi$: if $C$ is constant then this has the exact solution

$$\psi = \psi(x - Ct) \tag{73}$$

and so any pulse moves with speed $\frac{dx}{dt} = C$. Any nonhomogeneous term corresponds to a source which adds or removes energy from the system. Then Eq. (70) tells us that the flux in the $N$ direction ($\Phi_\ell$) is naturally undiminished as it flows along a (null) surface of constant $v$ and increasing $\rho$. However the interaction with the flux in the $\ell$ direction can cause it to increase or decrease. Similarly Eq. (71) describes the flow of the flux in the $\ell$ direction ($\Phi_N$) along a surface of constant $\rho$ and increasing $v$. Rewriting with respect to the affine derivative (see the Appendix B) $D_v = \partial_v + \kappa$ it becomes

$$D_v \Phi_N + C \Phi_{N,\rho} = -\frac{R_N \Phi_\ell}{R}. \tag{74}$$

Then, as might be expected, $\Phi_N$ naturally flows with coordinate speed $C$ (recall that $\ell = \frac{\partial}{\partial v} + C \frac{\partial}{\partial \rho}$ so this is the speed of outgoing light relative to the coordinate system) but its strength can be augmented or diminished by interactions with the outward flux.

### A. System of first order PDEs

Together Eqs. (70) and (71) constitute a first-order system of partial differential equations (PDEs) for the scalar field. We now restructure the gravitational field equations in the same way.

First with respect to $\Phi_\ell$ and $\Phi_N$ the constraint equations (14)–(16) on constant $\rho$ surfaces become

$$R_{,v} = R_\ell - C R_N, \tag{75}$$

$$R_{\ell,v} = \kappa R_\ell + \frac{C(1 + 2R_\ell R_N)}{2R} - \frac{\Phi_\ell^2}{R}, \tag{76}$$

$$R_{N,v} = -\kappa R_N - \frac{(1 + 2R_\ell R_N)}{2R} + \frac{C\Phi_N^2}{R} \tag{77}$$

while the "time"-evolution equations (17)–(19) are

$$R_{,\rho\rho} = -\frac{\Phi_N^2}{R}, \tag{78}$$

$$(RR_\ell)_{,\rho} = -\frac{1}{2}, \tag{79}$$

$$C_{,\rho\rho} = \frac{1 + 2R_\ell R_N}{R^2} - \frac{2\Phi_\ell \Phi_N}{R^2}. \tag{80}$$

Two of these equations can be simplified. First, integrating Eq. (79) from $\rho = 0$ on which $R_\ell \overset{H}{=} 0$ we find

$$R_\ell = -\frac{\rho}{2R}. \tag{81}$$

This can be substituted into Eq. (76) to turn it into an algebraic constraint

$$C = 2\Phi_\ell^2 - 2R_\ell(\kappa R + R_\ell). \tag{82}$$

Despite these simplifications, the presence of interacting outward and inward matter fluxes means that in contrast to the dust examples, this is truly a set of coupled partial differential equations. Hence we can expect that the matter and spacetime dynamics will be governed by off-horizon data in addition to data at $\rho = 0$.

We reformulate as a system of first-order PDEs in the following way. First designate

$$\{R, R_N, \kappa, \Phi_\ell, \Phi_N\} \tag{83}$$

as the *primary variables*. The *secondary variables* $\{R_\ell, C\}$ are defined by Eqs. (81) and (82) in terms of the primaries.

Next on $\rho = \text{const}$ surfaces the primary variables are constrained by

$$R_{,v} = R_\ell - C R_N \quad \text{and} \tag{84}$$

$$R_{N,v} = -\kappa R_N - \frac{1}{2R}(1 + 2R_\ell R_N - 2C\Phi_N^2) \tag{85}$$

along with the scalar flux equation (71) while their time evolution is governed by

$$R_{,\rho} = R_N, \tag{86}$$

$$R_{N,\rho} = -\frac{\Phi_N^2}{R}, \tag{87}$$

$$\kappa_{,\rho} = \frac{1}{R^2}(1 + 2R_\ell R_N - 2\Phi_\ell \Phi_N), \tag{88}$$

$$\Phi_{\ell,\rho} = -\frac{R_\ell \Phi_N}{R}. \tag{89}$$

We now consider how all of these equations may be used to integrate final data. The scheme is closely related to that used in Ref. [27].

### B. Final data on $\bar{H}$ and $\bar{\mathcal{N}}$

In line with the depiction in Fig. 1(b), we specify final data on $H \cup \mathcal{N}$ or rather on the sections $\bar{H} \cup \bar{\mathcal{N}}$ where

$$\bar{H} = \{(0, v) \in H : v_i \le v \le v_f\} \quad \text{and}$$
$$\bar{\mathcal{N}} = \{(\rho, v_f) \in \mathcal{N} : \rho_i \le \rho \le 0\}. \tag{90}$$

Their intersection sphere is $\bar{H} \cap \bar{\mathcal{N}} = (0, v_f)$. Here and in what follows we suppress the angular coordinates.

The final data is

$$\bar{H}: \Phi_\ell$$
$$\bar{\mathcal{N}}: \Phi_N \quad \text{and}$$
$$\bar{H} \cap \bar{\mathcal{N}}: R = R_o. \tag{91}$$

$\Phi_\ell$ on $\bar{H}$ is a function of $v$ while $\Phi_N$ on $\bar{\mathcal{N}}$ is a function of $\rho$. $R_o$ is a single number.

Further on $H$ we have

$$R_\ell \overset{H}{=} 0 \quad \text{and} \quad R_N \overset{H}{=} -1 \tag{92}$$

where the null vectors are scaled in the usual way and, as before, the notation $\overset{H}{=}$ indicates that all quantities on both sides of the equality are evaluated on $H$.

This data can be used to evaluate $C$ and $R$ on $\bar{H}$. From Eqs. (82) and (84)

$$C \overset{H}{=} 2\Phi_\ell^2 \quad \text{and} \tag{93}$$

$$R \overset{H}{=} R_o + 2\int_{v_f}^{v} \Phi_\ell^2 \mathrm{d}v. \tag{94}$$

This is shown in Fig. 4. To find $\Phi_N$ on $\bar{H}$ we would need to solve

$$\Phi_{N,v} + \frac{1}{2R}(1 - 4\Phi_\ell^2\Phi_N^2)\Phi_N \overset{H}{=} -2\Phi_\ell^2\Phi_{N,\rho} + \frac{\Phi_\ell}{R} \tag{95}$$

which comes from Eq. (71) combined with the above results. However at this stage $\Phi_{N,\rho}$ is not known and so this can only be solved directly in the isolated $\Phi_\ell \overset{H}{=} 0$ case. There

$$\Phi_N^{\mathrm{iso}} \overset{H}{=} \Phi_{N_f} e^{-(v-v_f)/2R_o} \tag{96}$$

where $\Phi_{N_f} = \Phi_N(0, v_f)$. Equivalently (see Appendix B) $\Phi_N$ is affinely constant on an isolated horizon.

With $R_N = -1$, Eq. (77) tells us that

$$\kappa \overset{H}{=} \frac{1}{2R}(1 - 2C\Phi_N^2), \tag{97}$$

and so without $\Phi_N$ on $\bar{H}$ we also cannot determine this (away from isolation). However the corner $\bar{H} \cap \bar{\mathcal{N}}$ is an exception to that rule. There we know $\Phi_\ell$, $\Phi_N$ and $R_o$ and so

$$\kappa \overset{\bar{H}\cap\bar{\mathcal{N}}}{=} \frac{1}{2R_o}(1 - 4\Phi_\ell^2\Phi_N^2). \tag{98}$$

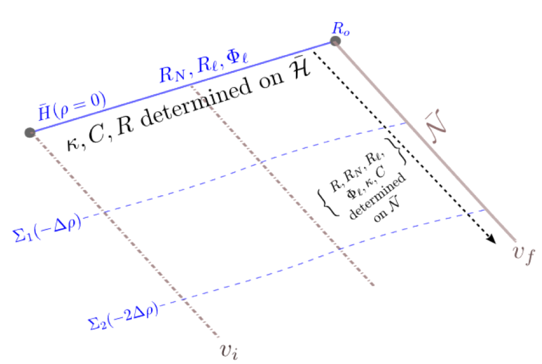


FIG. 4. The constraint equations along with initial conditions on the horizon, i.e., $R_\ell \overset{H}{=} 0$, $R_N \overset{H}{=} -1$ determine $\kappa$, $C$ and $R$ on $\bar{H}$.

The situation is less complicated on $\bar{\mathcal{N}}$. There with $\Phi_N$ as known data and final values known for all quantities on $\bar{H} \cap \bar{\mathcal{N}}$ all other quantities can be calculated in order.

(i) Solve Eqs. (86) and (87) for $R$ and $R_N$.
(ii) Calculate $R_\ell$ from Eq. (81).
(iii) Solve Eq. (89) for $\Phi_\ell$.
(iv) Solve Eq. (88) for $\kappa$.
(v) Calculate $C$ from Eq. (82).

We then have all data on $\bar{\mathcal{N}}$.

### C. Integrating from the final data

We now consider how that data can be integrated into the causal past of $\bar{H} \cup \bar{\mathcal{N}}$. The basic steps in the integration scheme are demonstrated in a simple numerical integration based on Euler approximations. This scheme alternates between using steps i)–v) to integrate data down the characteristics of constant $v$ followed by an application of Eq. (71) to calculate $\Phi_N$ on the next characteristic.

In more detail, assume a discretization $\{v_m, \rho_n\}$ (with $m$ and $n$ at their maxima along the final surfaces) by steps $\Delta v$ and $\Delta\rho$. Then if all data is known along a surface $v_{m+1}$ and $R$ and $\Phi_\ell$ are known everywhere on $\bar{H}$:

(a) Use the knowledge of $\Phi_N$ on $v_{m+1}$ to calculate $\Phi_{N,\rho}$.
(b) Use Eq. (71) at $(v_m, \rho_n)$ to find $\Phi_{N,v}$. Then

$$\Phi_N(v_m, \rho_n) \approx \Phi_N(v_{m+1}, \rho_n) - \Phi_{N,v}(v_{m+1}, \rho_n)\Delta v. \tag{99}$$

(c) Apply Eq. (97) to calculate $\kappa$ at $(v_m, 0)$.
(d) Use Eqs. (86)–(89) to integrate the values of $R_{N,\rho}$, $\kappa_{,\rho}$ and $\Phi_{\ell,\rho}$ out along the $v = v_m$ characteristic as for the initial data.

This can then be repeated marching all the way along $\bar{H}$ as shown in Fig. 5.

This is how we would proceed for general cases. However those general studies will be left for a future

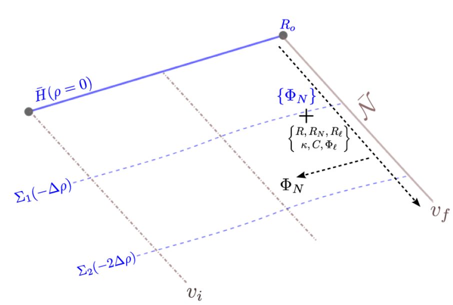


FIG. 5. Evolving $\Phi$ in the $-\frac{\partial}{\partial v}$ direction.

paper. Here instead we will focus on spacetime near a slowly evolving horizon. There, as will be seen in the next section, $\Phi_{N,\rho}$ is negligible and it becomes possible to integrate along surfaces of constant $v$.

It may not be immediately obvious how this integration scheme obeys causality and what restricts it to determining points inside the domain of dependence. This is briefly discussed in Appendix A.

### D. Spacetime near a slowly evolving horizon

We now apply the formalism to a concrete example: weak scalar fields near the horizon. Physically the black hole will be close to equilibrium and hence the horizon will evolve slowly in the sense of Refs. [17,35].

"Near horizon" means that we expand all quantities as Taylor series in $\rho$ and keep terms up to order $\rho^2$. "Weak scalar field" means that we assume

$$\Phi_N, \;\; \Phi_\ell \sim \frac{\varepsilon}{R} \tag{100}$$

and then expand the terms of the Taylor series up to order $\epsilon^2$. To order $\epsilon^0$ the spacetime will be vacuum (and Schwarzschild), order $\epsilon^1$ will be a test scalar field propagating on the Schwarzschild background and order $\epsilon^2$ will include the backreaction of the scalar field on the geometry.

#### 1. Expanding the equations

We expand all quantities as Taylor series in $\rho$. That is for $X \in \{R, R_N, R_\ell, \kappa, C, \Phi_\ell, \Phi_N\}$

$$X(v,\rho) = \sum_{n=0}^{\infty} \frac{\rho^n X^{(n)}(v)}{n!} \tag{101}$$

with

$$R_N^{(n)} = R^{(n+1)} \quad \text{and} \quad \kappa^{(n)} = C^{(n+1)}. \tag{102}$$

The free final data is $\Phi_\ell^{(0)}$ on $\bar{H}$, $R_o$ on $\bar{H} \cap \bar{\mathcal{N}}$ and the Taylor-expanded

$$\Phi_{N_f}(\rho) = \sum_{n=0}^{\infty} \frac{\rho^n}{n!} \Phi_{N_f}^{(n)} \tag{103}$$

on $\bar{\mathcal{N}}$. Following Ref. [37] we give names to special cases of this free data.

(i) *Out modes*: no flux through $\bar{H}$ ($\Phi_\ell^{(0)} = 0$), nonzero flux through $\bar{\mathcal{N}}$ ($\Phi_N^{(n)} \neq 0$ for some $n$).

(ii) *Down modes*: nonzero flux through $\bar{H}$ ($\Phi_\ell^{(0)} \neq 0$), zero flux through $\bar{\mathcal{N}}$ ($\Phi_N^{(n)} = 0$ for all $n$).

From the free data we construct the rest of the final data on $\bar{H}$. Equations (93) and (97) give

$$C^{(0)} = 2\Phi_\ell^{(0)^2}, \tag{104}$$

$$C^{(1)} = \kappa^{(0)} \approx \frac{1}{2R^{(0)}}. \tag{105}$$

Here and in what follows the $\approx$ indicates that terms of order $\epsilon^3$ or higher have been dropped. Further by our gauge choice

$$R_N^{(0)} = R^{(1)} = -1 \tag{106}$$

and so from Eq. (94)

$$R^{(0)} = R_o + \int_{v_f}^{v} C^{(0)} \mathrm{d}v. \tag{107}$$

This is an order-$\epsilon^2$ correction as long as the interval of integration is small relative to $1/\epsilon$.

The last piece of final data on $\bar{H}$ is $\Phi_N^{(0)}$ and comes from the first-order differential equation (95)

$$\frac{\mathrm{d}\Phi_N^{(0)}}{\mathrm{d}v} + \frac{\Phi_N^{(0)}}{2R_o} \approx \frac{\Phi_\ell^{(0)}}{R_o} \tag{108}$$

which has the solution

$$\Phi_N^{(0)} = \Phi_{N_f}^{(0)} e^{(v_f - v)/2R_o} + e^{-v/2R_o} \int_{v_f}^{v} e^{\tilde{v}/2R_o} \Phi_\ell^{(0)} \mathrm{d}\tilde{v} \tag{109}$$

in which the free data $\Phi_{N_f}^{(0)}$ came in as a boundary condition. Note that scalar fields that start small on the boundaries remain small in the interior, again as long as the integration time is short compared to $1/\epsilon$. We assume that this is the case.

From the final data, the black hole is close to equilibrium and the horizon is slowly evolving to order $\epsilon^2$. That is, the expansion parameter [17,35]

$$C\left(\frac{1}{2}\theta_{(N)}^2 + G_{ab}N^a N^b\right) \approx \left(\frac{4\Phi_\ell^2}{R^2}\right) \sim \frac{4\epsilon^2}{R^2}. \tag{110}$$

Further we already have the first-order expansion of $C$:

$$C \approx 2\Phi_\ell^{(0)^2} + \frac{\rho}{2R_o}. \tag{111}$$

That is (to first order) there is a null surface at

$$\rho_{\mathrm{EHC}} \approx -4R_o \Phi_\ell^{(0)^2}. \tag{112}$$

This null surface is the event horizon candidate discussed in Ref. [34]: if the horizon evolves slowly throughout its future evolution and ultimately transitions to isolation then the event horizon candidate is the event horizon.

Moving off the horizon to calculate up to second order in $\rho^2$, from Eqs. (86) and (87) we find

$$R_N^{(1)} = R^{(2)} \approx -\frac{\Phi_N^{(0)^2}}{R_o}, \tag{113}$$

$$R_N^{(2)} \approx -\frac{\Phi_N^{(0)}(\Phi_N^{(0)} + 2R_o\Phi_N^{(1)})}{R_o^2} \tag{114}$$

and so from Eq. (81)

$$R_\ell^{(0)} = 0, \tag{115}$$

$$R_\ell^{(1)} = -\frac{1}{2R^{(0)}}, \tag{116}$$

$$R_\ell^{(2)} = -\frac{1}{R^{(0)^2}}. \tag{117}$$

Note that the last two terms will include terms of order $\epsilon^2$ once the Eq. (107) integration is done to calculate $R^{(0)}$.

From Eq. (89) we can rewrite $\Phi_\ell^{(n)}$ terms with respect to $\Phi_N^{(n)}$ ones:

$$\Phi_\ell^{(1)} = 0, \tag{118}$$

$$\Phi_\ell^{(2)} \approx \frac{\Phi_N^{(0)}}{2R_o^2}. \tag{119}$$

The vanishing linear-order term reflects the fact that close to the horizon (where $R_\ell = 0$) the inward flux decouples from the outward flux (89) and so freely propagates into the black hole. Physically this means that (to first order in $\rho$ near the horizon) the horizon flux is approximately equal to the "near-horizon" flux.

Next, from Eq. (88)

$$\kappa^{(1)} = C^{(2)} \approx \frac{1}{R^{(0)^2}} - \frac{2\Phi_\ell^{(0)}\Phi_N^{(0)}}{R_o^2} \quad \text{and} \tag{120}$$

$$\kappa^{(2)} \approx \frac{3}{R^{(0)^2}} - \frac{2\Phi_\ell^{(0)}(2\Phi_N^{(0)} + R_o\Phi_N^{(1)})}{R_o^2}. \tag{121}$$

Again keep in mind that the $R^{(0)}$ terms will be corrected to order $\epsilon^2$ from Eq. (107).

Finally these quantities may be substituted into Eq. (71) to get differential equations for the $\Phi_N^{(n)}$:

$$\frac{\mathrm{d}\Phi_N^{(1)}}{\mathrm{d}v} + \frac{\Phi_N^{(1)}}{R_o} \approx \frac{\Phi_\ell^{(0)}}{R_o^2} - \frac{\Phi_N^{(0)}}{R_o^2}, \tag{122}$$

$$\frac{\mathrm{d}\Phi_N^{(2)}}{\mathrm{d}v} + \frac{3\Phi_N^{(2)}}{2R_o} \approx \frac{2\Phi_\ell^{(0)}}{R_o^3} - \frac{5\Phi_N^{(0)}}{2R_o^3} - \frac{3\Phi_N^{(1)}}{R_o^2}. \tag{123}$$

Like Eq. (109) these are easily solved with an integrating factor and respectively have $\Phi_{N_f}^{(1)}$ and $\Phi_{N_f}^{(2)}$ as boundary conditions.

Note the important simplification in this regime that enables these straightforward solutions, namely, the fact that $R_\ell \sim \rho$ has raised the $\rho$ order of the $\Phi_{N,\rho}$ terms. As a result we can integrate directly across the $\rho = \text{const}$ surfaces rather than having to pause at each step to first calculate the $\rho$ derivative. The $\Phi_{N_f}^{(n)}$ are final data for these equations. They can be solved order by order and then substituted back into the other expressions to reconstruct the near-horizon spacetime.

It is also important that the matter and geometry equations decompose cleanly in orders of $\epsilon$: we can solve the matter equations at order $\epsilon$ relative to a fixed background geometry and then use those results to solve for the corrections to the geometry at order $\epsilon^2$.

### 2. Constant inward flux

We now consider the concrete example of an affinely constant flux through $\bar{H}$ along with an analytic flux through $\bar{\mathcal{N}}$. Then by Appendix B

$$\Phi_\ell^{(0)} = \Phi_{\ell_f}^{(0)} e^V, \tag{124}$$

where $\Phi_{\ell_f}^{(0)}$ is the value of $\Phi_\ell^{(0)}$ at $v_f$ and $V = \frac{v - v_f}{2R_o}$ while $\Phi_{N_f}$ retains its form from Eq. (103).

We solve the equations for this data up to second order in $\rho$ and $\epsilon$. First for $\Phi_N^{(n)}$ equations we find

$$\Phi_N^{(0)} \approx (e^V - e^{-V})\Phi_{\ell_f}^{(0)} + e^{-V}\Phi_{N_f}^{(0)}, \tag{125}$$

$$\Phi_N^{(1)} \approx \frac{2\Phi_{\ell_f}^{(0)}}{R_o}(1 - e^{-2V}) + \frac{2\Phi_{N_f}^{(0)}}{R_o}(e^{-2V} - e^{-V}) + \Phi_{N_f}^{(1)} e^{-2V}, \tag{126}$$

$$\Phi_N^{(2)} \approx -\frac{\Phi_{\ell_f}^{(0)}}{4R_o^2}(e^V + 14e^{-V} - 48e^{-2V} + 33e^{-3V})$$

$$+ \frac{\Phi_{N_f}^{(0)}}{2R_o^2}(7e^{-V} - 24e^{-2V} + 17e^{-3V}) \tag{127}$$

$$+ \frac{6\Phi_{N_f}^{(1)}}{R_o}(e^{-3V} - e^{-2V}) + \Phi_{N_f}^{(2)} e^{-3V} \tag{128}$$

and so

$$\Phi_\ell^{(0)} = e^V \Phi_{\ell_f}^{(0)}, \tag{129}$$

$$\Phi_\ell^{(1)} = 0, \tag{130}$$

$$\Phi_\ell^{(2)} \approx \frac{\Phi_{\ell_f}^{(0)}}{2R_o^2}(e^V - e^{-V}) + \frac{\Phi_{N_f}^{(0)}}{2R_o^2}e^{-V}. \tag{131}$$

The scalar field equations are linear and so it is not surprising that to this order in $\epsilon$ each solution can be thought of as a linear combination of down and out modes.

However for the geometry at order $\epsilon^2$, down and out modes no longer combine in a linear way. These quantities can be found simply by substituting the $\Phi_\ell^{(n)}$ and $\Phi_N^{(n)}$ into the expression for $R^{(n)}$, $R_N^{(n)}$, $R_\ell^{(n)}$, $C^{(n)}$ and $\kappa^{(n)}$ given in the last section. They are corrected at order $\epsilon^2$ by flux terms that are quadratic in combinations of $\Phi_{\ell_f}^{(m)}$ and $\Phi_{N_f}^{(n)}$. The terms are somewhat messy and the details are not especially enlightening. Hence we do not write them out explicitly here.

### 3. $\bar{H}-\bar{\mathcal{N}}$ correlations

From the preceding sections it is clear that there does not need to be any correlation between the scalar field flux crossing $\bar{H}$ and that crossing $\bar{\mathcal{N}}$. These fluxes are actually free data. Any correlations will result from appropriate initial configurations of the fields. In this final example we consider a physically interesting case where such a correlation exists.

Consider quadratic affine final data (Appendix B) on $\bar{H} = \{(v,0): v_i < v < v_f\}$,

$$\Phi_\ell^{(0)} = a_0 e^V + a_1 e^{2V} + a_2 e^{3V} \tag{132}$$

for $V = v - v_f/2R_o$ along with similarly quadratic affine data on $\bar{\mathcal{N}}$,

$$\Phi_{N_f} = \Phi_{N_f}^{(0)} + \rho\Phi_{N_f}^{(1)} + \frac{\rho^2}{2}\Phi_{N_f}^{(2)}. \tag{133}$$

*A priori* these are uncorrelated but let us restrict the initial configuration so that $\Phi_N^{(n)}(v_i) = 0$. That is, there is no $\Phi_N$ flux through $v = v_i$.

Then the process to apply these conditions is, given the free final data on $\bar{H}$:

(i) Solve for the $\Phi_N^{(n)}$ from Eqs. (108), (122) and (123).

(ii) Solve $\Phi_N^{(n)}(v_i) = 0$ to find the $\Phi_{N_f}^{(n)}$ in terms of the $a_n$. These are linear equations and so the solution is straightforward.

(iii) Substitute the resulting expressions for $\Phi_N^{(n)}$ into results from the previous sections to find all other quantities.

These calculations are straightforward but quite messy. Here we only present the final results for $\Phi_{N_f}$:

$$\Phi_{N_f}^{(0)} \approx (1-e^{2V_i})a_0 + \frac{2a_1(1-e^{3V_i})}{3} + \frac{a_2(1-e^{4V_i})}{2}, \tag{134}$$

$$\Phi_{N_f}^{(1)} \approx \frac{2a_0(e^{2V_i} - e^{3V_i})}{R_o} + \frac{a_1(1+8e^{3V_i} - 9e^{4V_i})}{6R_o} + \frac{a_2(1+5e^{4V_i} - 6e^{5V_i})}{5R_o}, \tag{135}$$

$$\Phi_{N_f}^{(2)} \approx -\frac{a_0(1+14e^{2V_i} - 48e^{3V_i} + 33e^{4V_i})}{4R_o^2} - \frac{a_1(1+35e^{3V_i} - 135e^{4V_i} + 99e^{5V_i})}{15R_o^2} + \frac{a_2(1-35e^{4V_i} + 144e^{5V_i} - 110e^{6V_i})}{20R_o^2} \tag{136}$$

where $V_i = V(v_i)$. If $V_i$ is sufficiently negative that we can neglect the exponential terms, then

$$\Phi_{N_f}^{(0)} \approx a_0 + \frac{2a_1}{3} + \frac{a_2}{2},$$
$$\Phi_{N_f}^{(1)} \approx \frac{a_1}{6R_o} + \frac{a_2}{5R_o},$$
$$\Phi_{N_f}^{(2)} \approx -\frac{a_0}{4R_o^2} + -\frac{a_1}{15R_o^2} + \frac{a_2}{20R_o^2}. \tag{137}$$

In either case the flux through $\bar{H}$ fully determines the flux through $\bar{\mathcal{N}}$. The constraint at $v_i$ is sufficient to determine the Taylor expansion of the flux through $\bar{\mathcal{N}}$ relative to the expansion of the flux through $\bar{H}$. Though we only did this to second order in $\rho/v$ we expect the same process to fix the expansions to arbitrary order.

## V. DISCUSSION

In this paper we have begun building a formalism that constructs spacetime in the causal past of a horizon $\bar{H}$ and an intersecting ingoing null surface $\bar{\mathcal{N}}$ using final data on those surfaces. It can be thought of as a specialized characteristic initial value formulation and is particularly closely related to that developed in Ref. [28]. Our main interest has been to use the formalism to better understand the relationship between horizon dynamics and off-horizon fluxes. So far we have restricted our attention to spherical symmetry and so included matter fields to drive the dynamics.

One of the features of characteristic initial value problems is that they isolate free data that may be specified on each of the initial surfaces. Hence it is no surprise that the corresponding data in our formalism is also free and uncorrelated. We considered two types of data: inward-flowing null matter and massless scalar fields.

For the inward-flowing null matter, data on the horizon actually determines the entire spacetime running backwards along the ingoing null geodesics that cross $\bar{H}$. Physically this makes sense. This is the only flow of matter and so there is nothing else to contribute to the dynamics.

More interesting are the massless scalar field spacetimes. In that case, matter can flow both inwards and outwards and further inward-moving radiation can scatter outwards and vice versa. For the weak-field near-horizon regime that we studied most closely, the free final data is the scalar field flux through $\bar{H}$ and $\bar{\mathcal{N}}$ along with the value of $R$ at their intersection. Hence, as noted, these fluxes are uncorrelated. However we also considered the case where there was no initial flux of scalar field traveling "up" the horizon. In this case the coefficients of the Taylor expansion of the inward flux on $\bar{H}$ fully determined those on $\bar{\mathcal{N}}$ (though in a fairly complicated way). This constraint is physically reasonable: one would expect the dominant matter fields close to a black hole horizon to be infalling as opposed to traveling (almost) parallel to the horizon. It is hard to imagine a mechanism for generating strong parallel fluxes.

While we have so far worked in spherical symmetry the current work still suggests ways to think about the horizon-$\mathcal{I}^+$ correlation problem for general spacetimes. For a dynamic nonspherical vacuum spacetime, gravitational wave fluxes will be the analogue of the scalar field fluxes of this paper and almost certainly they will also be free data. Then any correlations will necessarily result from special initial configurations. However as in our example these may not need to be very exotic. It may be sufficient to eliminate strong outward-traveling near-horizon fluxes. In future works we will examine these more general cases in detail.

## ACKNOWLEDGMENTS

This work was supported by NSERC Grants No. 2013-261429 and No. 2018-04873. We are thankful to Jeff Winicour for discussions on characteristic evolution during the Atlantic General Relativity Workshop and Conference at Memorial University. I. B. would like to thank Abhay Ashtekar, José-Luis Jaramillo and Badri Krishnan for discussions during the "Focus Session on Dynamical Horizons, Binary Coalescences, Simulations and Waveforms" at Penn State. Bradley Howell pointed out a correction to our general integration scheme which is now incorporated in Secs. IV B and IV C.

## APPENDIX A: CAUSAL PAST OF $\bar{H} \cup \bar{\mathcal{N}}$

In this Appendix we consider how the general integration scheme for the scalar field spacetimes of Sec. IV "knows" how to stay within the past domain of dependence of $\bar{H} \cup \bar{\mathcal{N}}$.

First, it is clear how the process develops spacetime up to the bottom left-hand null boundary ($v = v_i$) of the past domain of dependence. The bottom right-hand boundary is a little more complicated but follows from the advection form of the $\Phi_{N,v}$ equation (74). Details will depend on the exact numerical scheme but the general picture is as follows.

Assume that we have discretized the problem so that we are working at points $(v_j, \rho_k)$. Then in using Eq. (74) to move from a surface $v_i$ to $v_{i-1}$, the Courant-Friedrichs-Lewy (CFL) condition (common to many hyperbolic equations) tells us that the maximum allowed $\Delta v$ is

$$\Delta v < \frac{\Delta\rho}{C}, \tag{A1}$$

where $\Delta\rho$ is the coordinate separation of the points that we are using to calculate the right-hand side of Eq. (74).

Then, as shown in Fig. 6, the discretization progressively loses points from the bottom right of the diagram: they are outside of the domain of dependence of the individual points being used to determine them. For example if we are using a centred derivative so that

$$\Phi_{N,\rho} \approx \frac{\Phi_N(v_j, \rho_{k+1}) - \Phi_N(v_j, \rho_{k-1})}{2\Delta\rho} \tag{A2}$$

then we need adjacent points as shown in Fig. 6.

The lower-right causal boundary of Fig. 1 is then enforced by a combination of the end points of $\bar{\mathcal{N}}$ and the CFL condition as shown in Fig. 7. Points are progressively lost as they require greater than the maximum allowed $\Delta v$. The numerical past domain of dependence necessarily lies inside the analytic domain. The coarseness

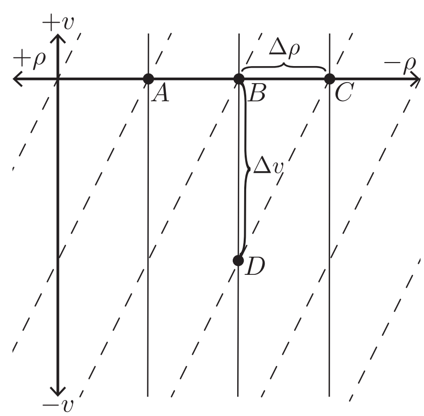


FIG. 6. Causality restrictions on $\Delta v$: the CFL condition restricts the choice of $\Delta v$ to ensure that attempted numerical evolutions respect causality. In this figure the $\rho$ and $v$ coordinates are drawn to be perpendicular to clarify the connection with the usual advection equation: to compare to other diagrams rotate about 45° clockwise and skew so coordinate curves are no longer perpendicular. The dashed lines are null and have slope $C$ in this coordinate system. If data at points $A$, $B$ and $C$ are used to determine $\Phi_{N,\rho}$ then the size of the discrete $v$ evolution is limited to lie inside the null line from point $C$. The largest $\Delta v$ allowed by the restriction evolves to $D$.

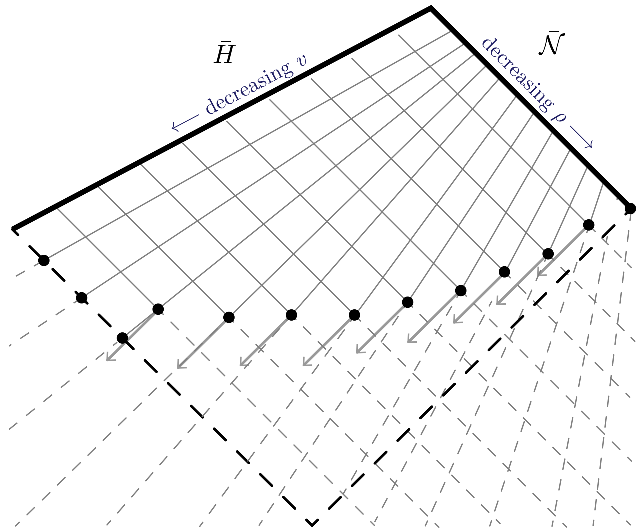


FIG. 7. A cartoon showing the CFL-limited past domain of dependence of $\bar{H} \cup \bar{\mathcal{N}}$. Null lines are now drawn at 45° so the analytic past domain of dependence is bound by the heavy dashed null lines running back from the ends of $\bar{H}$ and $\bar{\mathcal{N}}$. A (very coarse) discretization is depicted by the gray lines and the region that cannot be determined with dashed lines. The boundary points of that region are heavy dots.

of the discretization in the figure dramatizes the effect: a finer discretization would keep the domains closer.

## APPENDIX B: AFFINE DERIVATIVES AND FINAL DATA

The off-horizon $\rho$ coordinate in our coordinate system is affine while $v$ is not. However, as seen in the main text, when considering the final data on $\bar{H}$ it is more natural to work relative to an affine parameter. This is somewhat complicated because $\Phi_\ell$ and $\Phi_N$ are respectively linearly dependent on $\ell$ and $N$ and the scaling of those vectors is also tied to coordinates via Eqs. (1), (2) and (6). In this Appendix we will discuss the affine parametrization of the horizon and the associated affine derivatives for various quantities.

Restricting our attention to an isolated horizon $\bar{H}$ with $\kappa = \frac{1}{2R_o}$, consider a reparametrization

$$\tilde{v} = \tilde{v}(v). \tag{B1}$$

Then

$$\frac{\partial}{\partial v} = \frac{\mathrm{d}\tilde{v}}{\mathrm{d}v}\frac{\partial}{\partial \tilde{v}} \tag{B2}$$

and so

$$\ell = e^V \tilde{\ell} \quad \text{and} \quad N = e^{-V}\tilde{N} \tag{B3}$$

where we have defined $V$ so that $e^V = \frac{\mathrm{d}\tilde{v}}{\mathrm{d}v}$. Hence

$$\tilde{\kappa} = -\tilde{N}_b \tilde{\ell}^a \nabla_a \tilde{\ell}^b = e^{-V}\left(\kappa - \frac{\mathrm{d}V}{\mathrm{d}v}\right) \tag{B4}$$

and so for an affine parametrization ($\kappa = \partial_v V$)

$$e^V = \exp\left(\frac{v - v_f}{2R_o}\right) \tag{B5}$$

for some $v_f$ and

$$\tilde{v} - \tilde{v}_o = 2R_o e^V \tag{B6}$$

for some $\tilde{v}_o$. The $v_f$ freedom corresponds to the freedom to rescale an affine parametrization by a constant multiple while the $\tilde{v}_o$ is the freedom to set the zero of $\tilde{v}$ wherever you like.

Now consider derivatives with respect to this affine parameter. For a regular scalar field

$$\frac{\mathrm{d}f}{\mathrm{d}\tilde{v}} = e^{-V}\frac{\mathrm{d}f}{\mathrm{d}v}. \tag{B7}$$

However in this paper we are often interested in scalar quantities that are defined with respect to the null vectors:

$$\Phi_\ell^{(0)} = e^V \Phi_{\tilde{\ell}}^{(0)} \quad \text{and} \quad \Phi_N^{(0)} = e^{-V}\Phi_{\tilde{N}}^{(0)}. \tag{B8}$$

Then

$$\frac{\mathrm{d}\Phi_{\tilde{\ell}}^{(0)}}{\mathrm{d}\tilde{v}} = e^{-V}\frac{\mathrm{d}}{\mathrm{d}v}(e^{-V}\Phi_\ell^{(0)}) = e^{-2V}\left(\frac{\mathrm{d}\Phi_\ell^{(0)}}{\mathrm{d}v} - \kappa\Phi_\ell^{(0)}\right), \tag{B9}$$

$$\frac{\mathrm{d}\Phi_{\tilde{N}}^{(0)}}{\mathrm{d}\tilde{v}} = e^{-V}\frac{\mathrm{d}}{\mathrm{d}v}(e^{V}\Phi_N^{(0)}) = \frac{\mathrm{d}\Phi_N^{(0)}}{\mathrm{d}v} + \kappa\Phi_N^{(0)}. \tag{B10}$$

That is these quantities are affinely constant if

$$\Phi_\ell = e^V \Phi_{\ell_f}^{(0)} \quad \text{and} \quad \Phi_N = e^{-V}\Phi_{N_f}^{(0)} \tag{B11}$$

for some constants $\Phi_{\ell_f}^{(0)}$ and $\Phi_{N_f}^{(0)}$.

In the main text we write this affine derivative on $\bar{H}$ as $D_v$ with its exact form depending on the $\ell$ or $N$ dependence of the quantity being differentiated.

Finally at Eq. (132) we consider a $\Phi_\ell$ that is "affinely quadratic." By this we mean that

$$\begin{gathered} \Phi_{\tilde{\ell}} = A_o + A_1\tilde{v} + A_2\tilde{v}^2 \\ \Updownarrow \\ \Phi_\ell = a_o e^V + a_1 e^{2V} + a_2 e^{3V}, \end{gathered} \tag{B12}$$

where for simplicity we have set $\tilde{v}_o$ to zero (so that $v = 0$ is $\tilde{V} = 2R_o$) and absorbed the extra $2R_o$s into the $a_n$.

[1] Simulating extreme spacetimes, 2018, https://www.black-holes.org.
[2] S. W. Hawking and G. F. R. Ellis, *The Large Scale Structure of Space-Time*, Cambridge Monographs on Mathematical Physics (Cambridge University Press, Cambridge, England, 2011).
[3] K. S. Thorne, R. H. Price, and D. A. Macdonald, *Black Holes: The Membrane Paradigm*, edited by Kip S. Thorne (Yale University Press, New Haven, 1986).
[4] J. L. Jaramillo, R. P. Macedo, P. Moesta, and L. Rezzolla, Black-hole horizons as probes of black-hole dynamics I: Post-merger recoil in head-on collisions, Phys. Rev. D **85**, 084030 (2012).
[5] J. L. Jaramillo, R. P. Macedo, P. Moesta, and L. Rezzolla, Black-hole horizons as probes of black-hole dynamics II: Geometrical insights, Phys. Rev. D **85**, 084031 (2012).
[6] J. L. Jaramillo, R. P. Macedo, P. Moesta, and L. Rezzolla, Towards a cross-correlation approach to strong-field dynamics in Black Hole spacetimes, AIP Conf. Proc. **1458**, 158 (2011).
[7] L. Rezzolla, R. P. Macedo, and J. L. Jaramillo, Understanding the 'anti-kick' in the Merger of Binary Black Holes, Phys. Rev. Lett. **104**, 221101 (2010).
[8] A. Gupta, B. Krishnan, A. Nielsen, and E. Schnetter, Dynamics of marginally trapped surfaces in a binary black hole merger: Growth and approach to equilibrium, Phys. Rev. D **97**, 084028 (2018).
[9] J. B. Griffiths and J. Podolsky, *Exact Space-Times in Einstein's General Relativity*, Cambridge Monographs on Mathematical Physics (Cambridge University Press, Cambridge, England, 2009).
[10] A. Ashtekar, C. Beetle, O. Dreyer, S. Fairhurst, B. Krishnan, J. Lewandowski, and J. Wisniewski, Isolated Horizons and their Applications, Phys. Rev. Lett. **85**, 3564 (2000).
[11] S. A. Hayward, General laws of black hole dynamics, Phys. Rev. D **49**, 6467 (1994).
[12] A. Ashtekar, C. Beetle, and S. Fairhurst, Isolated horizons: A Generalization of black hole mechanics, Classical Quantum Gravity **16**, L1 (1999).
[13] A. Ashtekar, C. Beetle, and S. Fairhurst, Mechanics of isolated horizons, Classical Quantum Gravity **17**, 253 (2000).
[14] S. A. Hayward, General laws of black-hole dynamics, Phys. Rev. D **49**, 6467 (1994).
[15] A. Ashtekar and B. Krishnan, Dynamical horizons and their properties, Phys. Rev. D **68**, 104030 (2003).
[16] R. Bousso and N. Engelhardt, Proof of a New Area Law in General Relativity, Phys. Rev. D **92**, 044031 (2015).
[17] I. Booth and S. Fairhurst, The First Law for Slowly Evolving Horizons, Phys. Rev. Lett. **92**, 011102 (2004).
[18] T. W. Baumgarte and S. L. Shapiro, *Numerical Relativity: Solving Einstein's Equations on the Computer* (Cambridge University Press, Cambridge, England, 2010).
[19] J. Thornburg, Event and apparent horizon finders for $3+1$ numerical relativity, Living Rev. Relativity **10**, 3 (2007).
[20] O. Dreyer, B. Krishnan, D. Shoemaker, and E. Schnetter, Introduction to isolated horizons in numerical relativity, Phys. Rev. D **67**, 024018 (2003).
[21] G. B. Cook and B. F. Whiting, Approximate killing vectors on S**2, Phys. Rev. D **76**, 041501 (2007).
[22] T. Chu, H. P. Pfeiffer, and M. I. Cohen, Horizon dynamics of distorted rotating black holes, Phys. Rev. D **83**, 104018 (2011).
[23] G. Lovelace *et al.*, Nearly extremal apparent horizons in simulations of merging black holes, Classical Quantum Gravity **32**, 065007 (2015).
[24] R. Owen, A. S. Fox, J. A. Freiberg, and T. P. Jacques, Black hole spin axis in numerical relativity, Phys. Rev. D **99**, 084031 (2019).
[25] A. D. Rendall, Reduction of the characteristic initial value problem to the Cauchy problem and its applications to the Einstein equations, Proc. R. Soc. Ser. A **427**, 221 (1990).
[26] R. K. Sachs, On the characteristic initial value problem in gravitational theory, J. Math. Phys. (N.Y.) **3**, 908 (1962).
[27] J. Winicour, Characteristic evolution and matching, Living Rev. Relativity **15**, 2 (2012).
[28] J. Winicour, Affine-null metric formulation of Einstein's equations, Phys. Rev. D **87**, 124027 (2013).
[29] T. Mädler and J. Winicour, Bondi-Sachs formalism, Scholarpedia **11**, 33528 (2016).
[30] C. Li and J. Lucietti, Transverse deformations of extreme horizons, Classical Quantum Gravity **33**, 075015 (2016).
[31] C. Li and J. Lucietti, Electrovacuum spacetime near an extreme horizon, arXiv:1809.08164.
[32] B. Krishnan, The spacetime in the neighborhood of a general isolated black hole, Classical Quantum Gravity **29**, 205006 (2012).
[33] J. Lewandowski and C. Li, Spacetime near Kerr isolated horizon, arXiv:1809.04715.
[34] I. Booth, Spacetime near isolated and dynamical trapping horizons, Phys. Rev. D **87**, 024008 (2013).
[35] I. Booth and S. Fairhurst, Isolated, slowly evolving, and dynamical trapping horizons: Geometry and mechanics from surface deformations, Phys. Rev. D **75**, 084019 (2007).
[36] I. Booth, L. Brits, J. A. Gonzalez, and C. Van Den Broeck, Marginally trapped tubes and dynamical horizons, Classical Quantum Gravity **23**, 413 (2006).
[37] *Black hole physics: Basic concepts and new developments*, edited by V. P. Frolov and I. D. Novikov (Springer, Dordrecht, 1998), Vol. 96.